

Effect of base roughness on size segregation in dry granular flows

Wei Zhou¹ · Zhiqiang Lai¹ · Gang Ma¹ · Lifu Yang¹ · Yuan Chen¹

Received: 15 April 2016 / Published online: 21 October 2016
© Springer-Verlag Berlin Heidelberg 2016

Abstract This paper presents simulations of dry granular flows along a sloping channel using the discrete element method. The kinetic sieving and squeeze expulsion theories are utilized to study the effects of base roughness on size segregation and the underlying mechanisms. Basal friction has a significant influence on flowing regimes inside the granular body, and a larger base friction accelerates the size segregation process. The front zone of the granular body is more likely to be collision dominated with increasing base friction; as a result, the energy dissipated by frictional shearing decreases, and damping energy due to particles collisions is enhanced. Meanwhile, granular flows become much looser, and collisions between particles increase rapidly. It is shown that the differences in the kinetics among grains of mixed sizes and the mechanical effects of particle contacts can explain the mechanism of size segregation. The parameter representing the intensity of particles exchange also increases as base friction increases. The forces acting on particles are also affected by base friction. The dimensionless contact force describing the contribution of contact channel-normal stress increases as base friction increases, which indicates

that a higher dispersive trend has developed inside the granular body.

Keywords Size segregation · Base roughness · Dry granular flows · Flowing regimes · Discrete element method

1 Introduction

Destructive granular flows, such as rock avalanches, debris flows and pyroclastic flows, tend to exhibit particle segregation. Particle segregation leads to a grading inversion, in which finer particles percolate down to the bottom of the flow, while coarser particles rise toward the top of the layers. Meanwhile, coarser particles in the top layers are then transported to the flow front, where they can be overrun and then recirculated, by particle segregation, to form a bouldery margin [1,2]. These natural phenomena have crucial effects on both the mobility of granular flows, and on the impact of granular flows on infrastructures [3,4]. Particle segregation also plays a key role in the compactness and stability of the dry granular flow deposits [5]. Therefore, understanding the fundamentals of particle segregation is of vital significance to improve the engineering control of debris flows and to assess the stability of these debris flow deposits.

A number of laboratory experiments and numerical simulations have been conducted to investigate the influencing factors and the underlying mechanisms of the granular segregation. Savage and Lun [6] observed that size difference induces particles to form a demixing distribution in the downward direction (normal to the channel surface) while particles flow along the slope channel. Granular density is also a primary factor affecting the segregation in dry granular flows [7]. The combined effects of size and density differences on the granular segregation have been investigated by several

✉ Gang Ma
magang630@whu.edu.cn

Wei Zhou
zw_mxx@163.com

Zhiqiang Lai
laizhiqiang0372@whu.edu.cn

Lifu Yang
yanglifu0598@163.com

Yuan Chen
yuancy_1013@whu.edu.cn

¹ State Key Laboratory of Water Resources and Hydropower Engineering Science, Wuhan University, Wuhan 430072, China

researchers [8,9]. No segregation occurs in the dry granular flows with particular combinations of radii and mass density ratios of two species [10,11]. Segregation also occurs in the granular mixture when grains differ in their restitution coefficients [12] or surface roughness [13].

In spite of the extensive numerical and experimental studies, there has been much work on developing continuum theories for size-particle segregation based on mixture theory. A review of the recent advances in developing these theories can be referred to Gray et al. [14]. Mixture theory defines a basic theoretical framework that includes partial and intrinsic variables and individual mass and momentum balances for each constituent. In the framework of mixture theory, the two-, three- and multi-constituent mixture theories for particle-size segregation and diffusive remixing have been proposed by Gray and Thornton [15], Gray and Chugunov [16], Thornton et al. [17], Gray and Ancey [18]. By coupling the depth-averaged avalanche models [19–21] with segregation models [15–17], depth-averaged segregation models have been developed to study the segregation-mobility feedback effects [1–3]. These continuum theories are able to accurately describe the evolution of the size distribution in size-segregation experiments [22,23] and numerical simulations [24–28], which offer insights into the nature of the size segregation.

The steady uniform flows have been extensively studied in both laboratory experiments [22] and numerical simulations [25–28], which provide simple approaches for researchers to verify, complement and develop continuum models for particle segregation. An experiment with steady uniform flows was performed to verify Gray and Chugunov's theory [16] for segregation and diffusive remixing in granular avalanches [22]. Using the discrete particle method (DPM), the steady-state simulations with binary mixtures were presented to determine the segregation parameter in the continuum model [25] and verify some of the assumptions of continuum segregation models in bi-dispersed chute flows [26]. Staron and Phillips [27] numerically analyzed the segregation time-scale in bi-disperse steady uniform flows and developed a simple model balancing lift and drag forces. Hill and Tan [28] extended the segregation theory accounting for the effects of both gravity and kinetic stress gradients and verified this theory using DEM simulations of steady-state flow dynamics. Simulating steady uniform flows allows the investigation of particle segregation can be more easily compared with the continuum theories.

Base roughness is a typical external factor affecting the flow dynamics. The flow processes of both the ordered and disordered flows are affected by the base roughness [29,30]. Regarding the granular flows in rotating semi-cylindrical chutes, the effect of base roughness on the flow behavior of mono-disperse granular particles is notable [31]. The influences of boundary roughness on the mechanical behav-

ior of granular materials [32] and flow behaviors in the hopper [33], funnel [34] and open channel [35] are also significant. Although the granular flows is sensitive to base roughness, the influence of base roughness on the particle segregation in granular flows, especially the transient flows with tri-disperse mixtures, has not been fully examined. The mechanism of how base roughness affects the flow regimes remains unknown.

The main purpose of this paper is to investigate the effects of base roughness on particle segregation and particle behavior in ternary mixtures. Discrete element simulations with calibrated parameters are conducted to simulate dry granular flows along the slope. Different friction coefficients between the walls and the particles are used to characterize the base roughness. Assuming that kinetic sieving and squeeze expulsion [6] are the dominant processes driving particle segregation, the fundamental relationship between particle segregation and base roughness is explored. The flow velocity distribution, shear rate, Savage number, the velocity differences of dissimilar sized particles, the relationship between the segregation parameters and the regimes of the transient flows, and the force differences acting on particles are analyzed to explain the underlying mechanism of particle segregation.

2 Numerical simulation of dry granular flows

2.1 Setup of the numerical model

An assembly of non-cohesive granular particles is simulated by a three-dimensional discrete element method code (Itasca PFC^{3D}). Figure 1 shows the numerical model setup and the deposited multi-layers. The numerical model is composed of a reservoir and a floor. The reservoir where particles rest is 2.1 m long, 0.4 m wide, 1.0 m deep and is constructed of elastic walls in PFC^{3D}. The two side walls and the bottom floor of the slope are infinitely large to guarantee that the particles can sufficiently segregate. The deposited multi-layers consist of three different sized particles (diameters of 0.02, 0.04, 0.08 m). The coarse particles are in the basal layer, whereas the medium and fine particles are in the middle and top layers, respectively. In each layer, the total mass of the particles is the same.

To investigate the effects of base roughness on size segregation of dry granular flows, the friction coefficients between the wall and the particles are set to different values (0.10–0.90), while the other parameters remain the same (as shown Table 1). The subscripts f, m and c denote the fine, medium and coarse particles, respectively. When the gate is removed, the static particles flow down along the floor of the slope due to gravity (9.80 m/s^2), and then size segregation occurs.

Note that the goal of this work is to qualitatively investigate how base roughness affects size segregation. Because

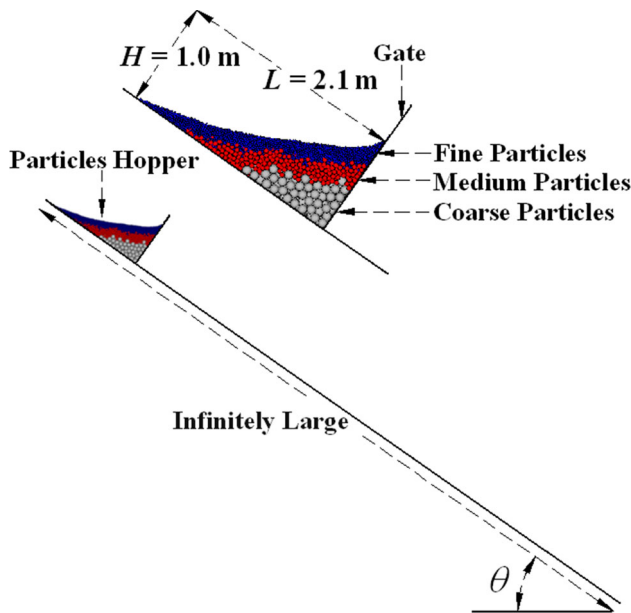


Fig. 1 Numerical model setup and deposited multi-layers

Table 1 Parameters of the numerical model

Parameter	Value
Slope angle	35°
Slope width	0.40 m
Mass of balls	450 kg
Density of each ball, ρ	2650 kg/m ³
Ball diameter, d_k (number of particles, N_k)	$d_f = 0.02$ m ($N_f = 13,500$) $d_m = 0.04$ m ($N_m = 1690$) $d_c = 0.08$ m ($N_c = 210$)
Stiffness of ball and wall	$k_n = k_t = 10^5$ N/m
Gravitational acceleration	9.80 m/s ²
Local damping, α	0.05
Normal viscous damping, β_n	0.20
Tangential viscous damping, β_t	0.20
Ball friction coefficient, μ_{ball}	0.58
Base friction coefficient, μ	0.10, 0.30, 0.50, 0.58, 0.70, 0.90

quantitative modeling is hard to conduct due to the complexity of natural granular flows. In order to acquire reasonable results, numerical parameters employed in the simulations are chosen from the references [36,37].

2.2 Contact law of the numerical model

A linear contact law is employed in the DEM simulation. The slip model is also implemented to allow slip to occur by limiting the shear force simultaneously. Figure 2 illustrates the particle–particle and particle-wall interactions, which includes a combination of an elastic spring, a fric-

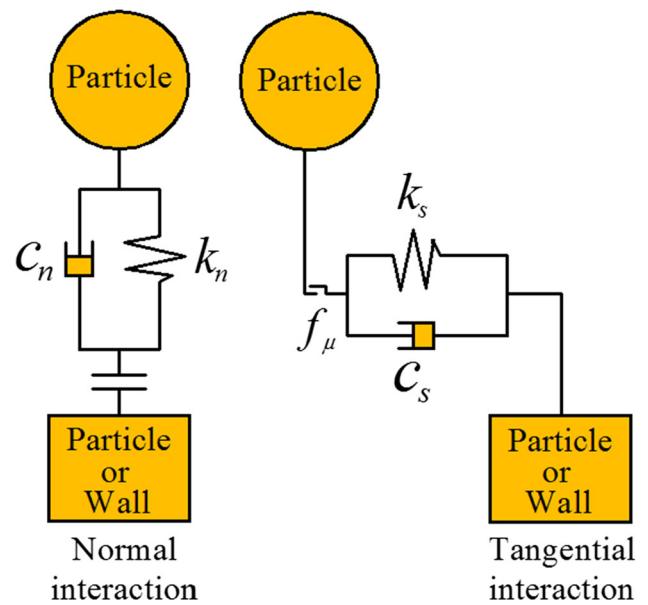


Fig. 2 Viscous damping activated at a contact with the linear contact model

tion slider and a dashpot. The combination represents elastic deformation, plastic deformation, friction and strain energy dissipation produced by interactions of particle–particle and particle-wall. The input damping is of great importance for matching the physical behavior of granular materials [38]. In PFC^{3D}, two types of damping, namely viscous damping and local damping, can be specified to dissipate the energy. The viscous damping is used to determine the damping force D_m , which is applied to each contact to describe the kinetic energy dissipated by particle collisions:

$$D_m = C_m |V_m| \quad (m = n, t) \tag{1}$$

where n and t represent the normal and tangential directions, respectively, V_m is the relative velocity in the normal or tangential direction of the contact and C_m is the dashpot damping coefficient.

The damping coefficient is not specified directly in PFC^{3D}. Instead, the critical damping ratio β_m is specified, and the damping constant satisfies [39]:

$$C_m = \beta_m C_m^{crit} \quad (m = n, t) \tag{2}$$

$$C_m^{crit} = 2M\omega_m = \beta_m 2\sqrt{Mk_m} \quad (m = n, t) \tag{3}$$

where ω_m is the natural frequency of the undamped system, k_m is the tangential contact stiffness, and M is the effective system mass.

In the collision dominant flows, particles under strong agitation sustain no interactions and flow into the air. Therefore, the energy dissipation due to the pore air viscosity should be considered. This type of energy dissipation can be mod-

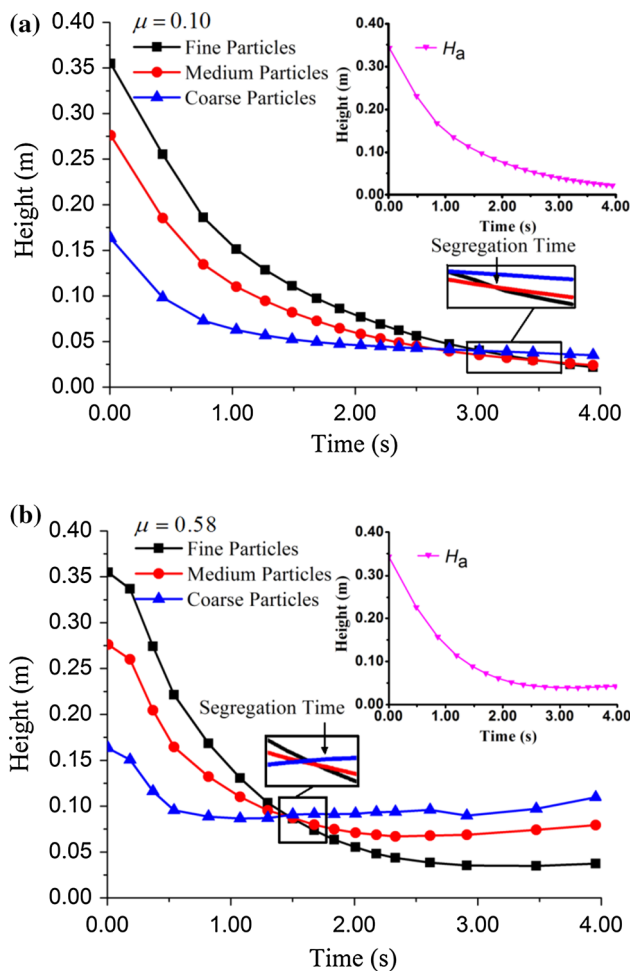


Fig. 3 Size segregation and average thickness of granular flows with different base friction coefficients during the flowing process: **a** base friction coefficient $\mu = 0.10$; **b** base friction coefficient $\mu = 0.58$

eled by the local damping. Many studies have shown that the local damping is necessary if there is significant rigid body motion of the particle system [37,39]. The damping force F_d is added to the equations of motion, which is proportional to the out-of-balance force F and in the contrary direction of the particle motion:

$$F_d = -\alpha |F| \text{sign}(v) \quad \text{sign}(y) = \begin{cases} +1 & \text{if } y > 0 \\ 0 & \text{if } y = 0 \\ -1 & \text{if } y < 0 \end{cases} \quad (4)$$

where α is the local damping coefficient, and v is the generalized velocity. The local damping is controlled by α in the simulation.

A combination of viscous damping and local damping is employed in the DEM simulation of dry granular flows. The damping coefficients adopted in the numerical model were calibrated by Zhou et al. [36,37]. Their research demonstrated that when local damping is 0.05 and viscous damping

is 0.20, the restitution coefficient of granular materials in the numerical model is approximately 0.50, which is close to that of real granular materials.

3 Simulation results and discussion

3.1 Effect of base roughness on size segregation

3.1.1 Particle segregation

When the gate is instantaneously pulled up, the particles behind it are released to flow down along the slope due to gravity. During the flowing process, the coarser particles rise to the top of the layer, and the finer particles deposit on the floor. The trajectories of three sized particles are captured using the corresponding averaged height. As the thicknesses at different positions of the granular flows are not the same, the average height of the flow is computed to reflect the overall thickness:

$$H_f = \sum_{i=1}^{N_f} \frac{H_i}{N_f} \quad H_m = \sum_{i=1}^{N_m} \frac{H_i}{N_m} \quad H_c = \sum_{i=1}^{N_c} \frac{H_i}{N_c}$$

$$H_a = \frac{\sum_{i=1}^{N_f+N_m+N_c} H_i}{N_f + N_m + N_c} \quad (5)$$

where H_i is the height of particle i away from the slope floor surface, H_a is the average thickness of the flow, N_f , N_m and N_c are the total numbers of fine, medium and coarse particles, respectively.

Figure 3 shows the evolution of the averaged height of three different sized particles during the flowing process along the slope under different base friction coefficients. Size segregation starts to develop at the very beginning of the simulation. The fine particles move to the bottom, whereas the coarse particles climb to the flow surface gradually. The inserted figure shows the evolution of the average height of the flow. It can be seen that the overall thickness of granular flows rapidly decreases to a very thinning layer. The thickness of granular flow with $\mu = 0.58$ decreases less slowly than that with $\mu = 0.10$ and then a slight bounce appears. This may be explained by that when μ enhanced, collisions between particles increase and the rebound height of particles increases.

The change of the volume fraction of particles at the base is also monitored. The particles in contact with the base wall are considered in the calculation of volume fraction near the base, which is implemented through a FISH code in PFC^{3D}. The volume fraction of particles in contact with the base wall

is computed as follows:

$$V_k = n_k \frac{\pi d_k^3}{6} \quad P_k = \frac{V_k}{\sum_i^{f,m,c} V_i} \quad (k = f, m, c) \quad (6)$$

where the subscripts f, m and c denote the fine, medium and coarse particles, respectively, V_k is the particle volume, d_k is the particle diameter, n_k is the number of different sized particles in contact with the base and P_k is the volume fraction of different sized particle.

It can be seen from Fig. 4 that the coarse particles first account for the largest percentage of those particles at the base due to the initial arrangement. After releasing the gate, some coarse particles fall to the base faster than the others due to shorter distance away from the base, which leads to the first increase of the percentage of coarse particles. Meanwhile, Size segregation starts to develop and becomes more and more obvious: the percentage of coarse particles at the base decreases to the smallest value while that of fine particles at the base becomes the largest. Larger μ accelerates the decline of the percentage of coarse particles at the base and makes the differences in the final percentages of different sized particles at the base more apparent.

3.1.2 Segregation time and effective coordination number

The segregation time is defined when the particles first inverse grade, i.e. the centers of mass are ordered so that the large are the highest, the medium are in the middle and the small are at the bottom. The segregation time of granular flows with different base friction coefficients is shown in Fig. 5. It can be seen that particles under the rough base have a higher segregation speed than the smooth base. However, this trend disappears when the base friction coefficient is greater than the inter-particle friction coefficient, which is 0.58 in all simulations.

It has been widely accepted that the void-filling process is the dominant mechanism for size segregation. Savage and Lun [6] performed experiments and found that the enhanced shearing between layers leads to a greater probability of seeing a hole that small particles may drop down into, which accelerates the size segregation. Compared with experiments, DEM has been instrumental in analyzing this phenomenon from the perspective of the particle scale information. The effective coordination number is used to demonstrate the relative degree of developing holes in dry granular flows. The effective coordination number, C_n , is defined as $C_n = 2C_{eff}/N$, where C_{eff} and N are the number of effective contacts and particles. The loss of contacts between particles is the prerequisite for developing the holes. Smaller coordination number C_n means that more contacts between particles are lost and there is a greater probability of developing holes that particles can drop through. The evolution of C_n for gran-

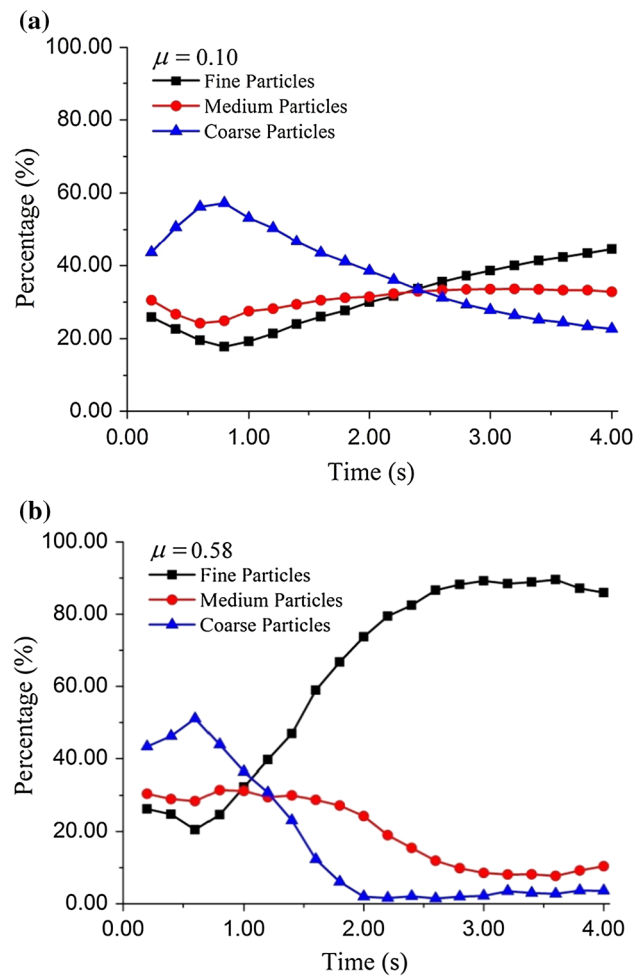


Fig. 4 Evolution of volume fraction of different sized particles at the base for granular flows with different base friction coefficients: **a** base friction coefficient $\mu = 0.10$; **b** base friction coefficient $\mu = 0.58$

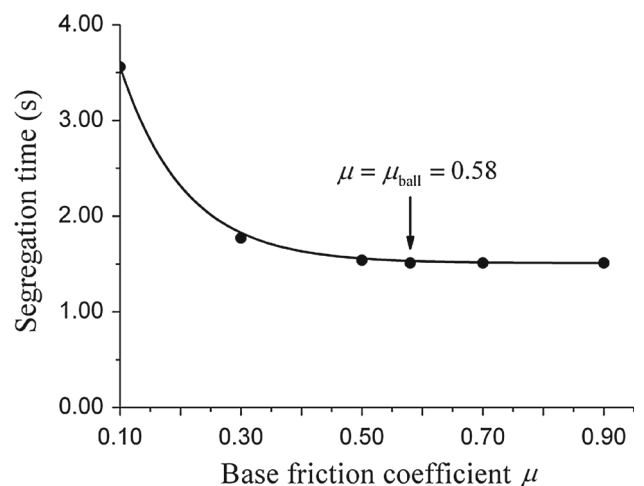


Fig. 5 Segregation time of granular flows with different base friction coefficients

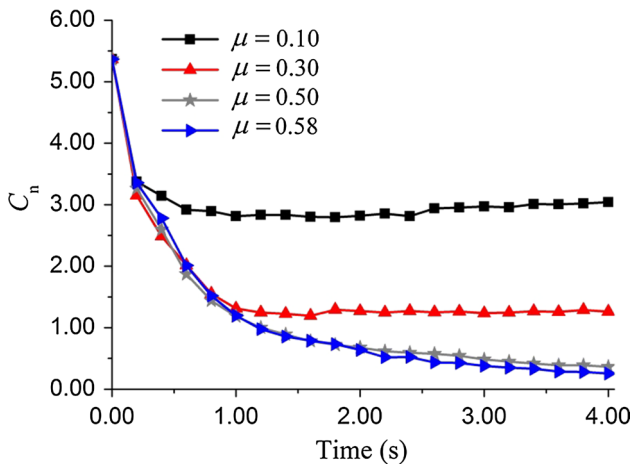


Fig. 6 Evolution of C_n for granular flows with different base friction coefficients

ular flows with different μ has been monitored in Fig. 6. It can be seen that larger μ leads to smaller C_n . For granular flows with $\mu = 0.50$ and 0.58 , the values of C_n are less than 1.00 . It indicates that most particles have lost contacts and became isolated, which will result in more holes in the granular bodies.

3.2 Flow regimes and kinetics affected by base roughness

3.2.1 Flow regimes

The velocity distributions inside granular flows are analyzed to investigate how base roughness may affect the flowing regimes. Figure 7 shows the computed velocity distribution along the height (normalized to the slope floor surface) and morphologies under different base roughness at the flowing time t of 1.00 s. The different symbols in Fig. 7 are used to distinguish the computed velocity distribution along the height at different positions inside the flowing body. Some symbols are expressed as the ratio of the current values divided by the corresponding initial or largest values. These normalized symbols in the figure are defined as follows:

$$L^* = \frac{L}{L_{\max}} \quad H^* = \frac{H}{H_{\max}} \quad U^* = \frac{U}{\sqrt{gL_0}} \quad (7)$$

where L^* is the ratio of the distance L away from the rear part divided by the whole length of flowing body L_{\max} along the slope floor, $L^* = 0.0$ at the rear part and $L^* = 1.0$ at the front head, H^* is the ratio of the flow thickness H divided by the largest flow thickness H_{\max} , U^* is the ratio of the traveling velocity U divided by $\sqrt{gL_0}$, where g is the gravity acceleration, and L_0 is the initial length of the deposited debris mass.

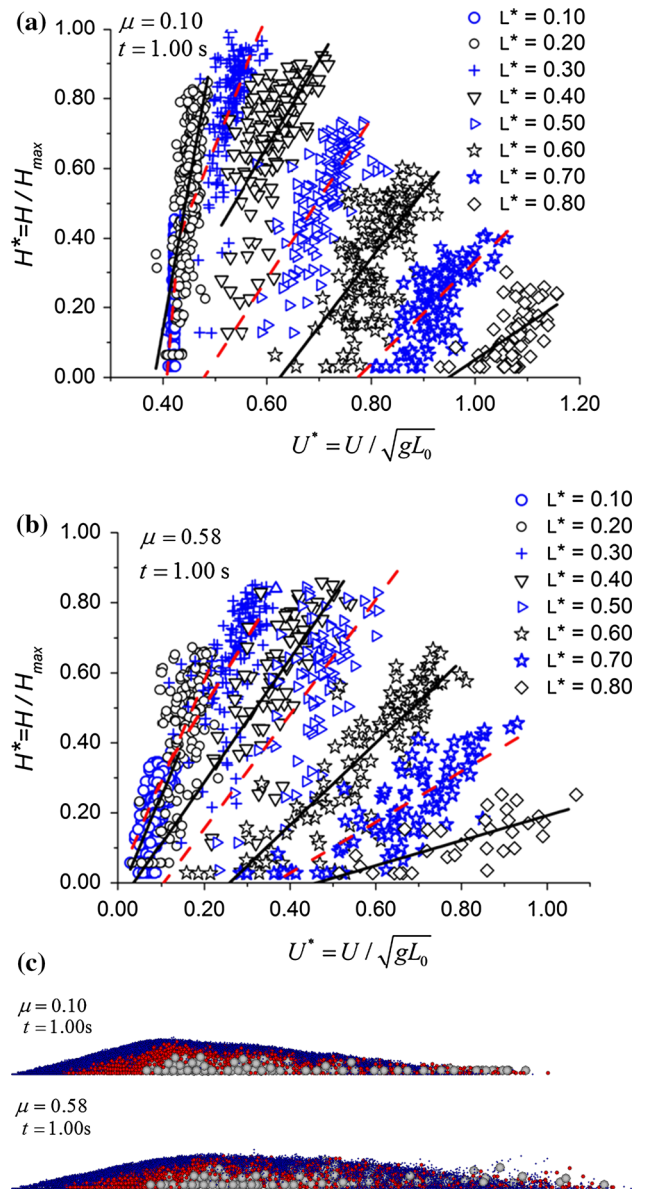


Fig. 7 Computed velocity distribution along the height and traveling direction and morphologies for granular flows with different base friction coefficients: **a** velocity distributions with base friction coefficient $\mu = 0.10$; **b** velocity distributions with base friction coefficient $\mu = 0.58$; **c** morphologies of granular flows with base friction coefficient $\mu = 0.10$ and 0.58

As shown in Fig. 7, the velocity profiles of the granular flows at each position can be well fitted by linear functions. The reciprocal value of tangential slope at each position represents the shear rate inside the flowing body, which increases from the rear part to the front head. The data points around the trend lines are scattered, which indicates that velocity fluctuation is developed inside the flowing body. The velocity of granular flows with base friction coefficient $\mu = 0.10$ is greater than that with $\mu = 0.58$ at the same part of the granular flows. At the flowing time t of 1.00 s, the morpholo-

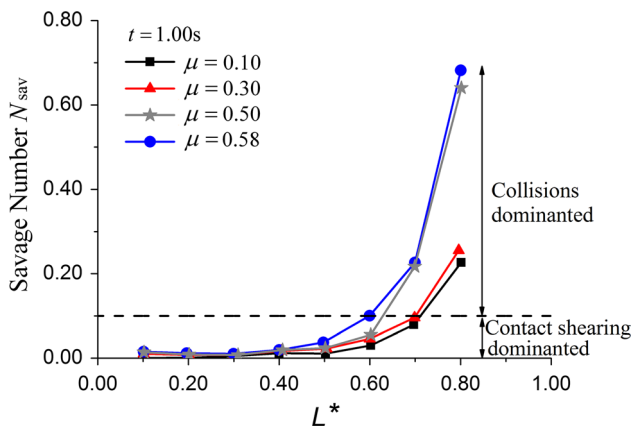


Fig. 8 Variation of the Savage number along the traveling direction for granular flows with different base friction coefficients

gies of granular flows with different base friction coefficients are also different. The flowing body with $\mu = 0.10$ features compact. When μ is greater, the flowing body (especially for the front part) becomes looser, and particles move apart.

To gain a deeper understanding of the effect of base roughness on the flowing regimes of granular flows, the Savage numbers of the granular flows with different base friction coefficients are monitored. The Savage number N_{sav} represents the relative significance of contact shearing and particle collisions (inertial effect) in the granular flows and is defined as follows [36,37,40,41]:

$$N_{sav} = \frac{\gamma^2 d^2}{gH\mu_{ball}} \tag{8}$$

where γ is the shearing rate, d is the particle diameter, and H is the flow thickness. According to the definition of the Savage number, contact shearing is dominant if $N_{sav} < 0.10$, whereas particle collisions are dominant if $N_{sav} \geq 0.10$. The Savage number N_{sav} is the square of the inertial number that also has been widely used.

Figure 8 shows that the change of the Savage number for granular flows with different base friction coefficients when the flowing time t is 1.00 s. It is found that the Savage numbers increase from the rear part to the front head of the granular flows. With increasing μ , the Savage numbers of the front part ($L^* \geq 0.50$) become greater, whereas the numbers of the rear part ($L^* < 0.50$) are almost the same. This implies that particles in the front part of the granular flows are more likely to be collision dominated, which coincides with the morphologies of granular flows in Fig. 7c.

Figure 9 shows the relative velocity distribution perpendicular to the floor surface for granular flows with different base friction coefficients. v_f , v_m and v_c in the figures are the

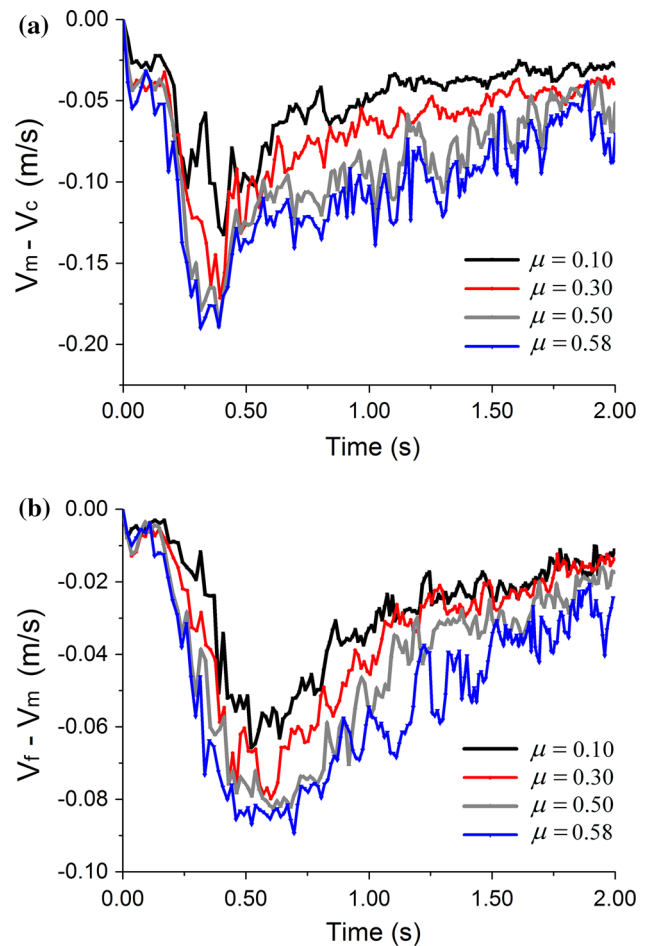


Fig. 9 Relative velocity distributions along the height for granular flows with different base friction coefficients: **a** relative velocity of medium and coarse particles; **b** relative velocity of fine and medium particles

bed-normal velocity component of fine, medium and coarse particles, respectively. The negative sign indicates that particles are moving to the slope floor. Compared with coarse particles, medium particles move to the slope floor more quickly. During the flowing process, the relative velocity between coarse particles and medium particles is denoted as $v_m - v_c$, which first increases to a maximum and then gradually decreases to a residual value. With increases in the base friction coefficient, the relative velocity increases. Fine particles possess higher values of the slope-normal velocity toward the slope compared with medium particles; $v_f - v_m$ experiences a similar variation as $v_m - v_c$. The difference in the bed-normal velocity component in fine, medium and coarse particles is the main factor that leads to size segregation. A greater base friction makes these velocity differences more obvious, thereby accelerating the size segregation process.

3.2.2 Connection with continuum theory

Gray and Ancy's theory [14, 18] showed that for a three constituent mixture, there are three segregation equations to describe the evolution of the size distribution, one of which can be eliminated by the summation condition $\phi^f + \phi^m + \phi^c = 1$. Substituting for ϕ^m by $\phi^m = 1 - \phi^f - \phi^c$, the two coupled equations can be given as follows [14, 18]:

$$\begin{aligned} \frac{\partial \phi^c}{\partial t} + \nabla \cdot (\phi^c \mathbf{u}) &= \frac{\partial}{\partial z} \left(-S_{cm} \phi^c (1 - \phi^c - \phi^f) - S_{cf} \phi^c \phi^f \right) \\ &\quad + \frac{\partial}{\partial z} \left(D_r \frac{\partial \phi^c}{\partial z} \right) \\ \frac{\partial \phi^f}{\partial t} + \nabla \cdot (\phi^f \mathbf{u}) &= \frac{\partial}{\partial z} \left(S_{cf} \phi^f \phi^c + S_{mf} \phi^f (1 - \phi^c - \phi^f) \right) \\ &\quad + \frac{\partial}{\partial z} \left(D_r \frac{\partial \phi^f}{\partial z} \right) \end{aligned} \tag{9}$$

where ∂ is used to indicate the partial derivative, ∇ is the gradient operator, z is the coordinate normal to the base, ϕ^f, ϕ^m, ϕ^c are the volume fraction of the fine, medium and coarse particles, respectively, \mathbf{u} is the bulk velocity field, S_{cm}, S_{mf}, S_{cf} are the non-dimensional segregation coefficient of two different constituents respectively and D_r is the non-dimensional diffusion coefficient:

$$S_{v\mu} = \frac{L'}{H'U'} q_{v\mu} \quad D_r = \frac{L'}{H'^2 U'} D \tag{10}$$

where L', H' and U' are the typical downstream length scale, typical thickness and typical downstream velocity magnitude, respectively, $q_{v\mu}$ is the segregation velocity of phase v relative to phase μ , and D is the diffusivity of the system.

The segregation parameters $q_{v\mu}$ and D are vital in this theory and they are not very easy to measure independently. Special attentions are given to explore the relationship between the segregation parameters and the regimes of transient flows. The segregation parameters q_{cm} (the same for q_{mf}), which is the relative velocity between coarse and medium particles or medium and fine particles, can be obtained from the Fig. 9. The system diffusivity D can be measured according to the expression as below [24]:

$$D = \left\langle \Delta z^2 / 2\Delta t \right\rangle \tag{11}$$

where Δz denotes a change in position during an time increment $\Delta t = 0.01$. The angle brackets denote an average made over all of the grains, and over some time. As the granular flows in the paper are transient flows, the system diffusivity D here is not a constant value. Different system diffusivities are computed every 0.20 s from the initial state to the flowing time of 2.00 s. For simplicity, the depth-averaged shear rate

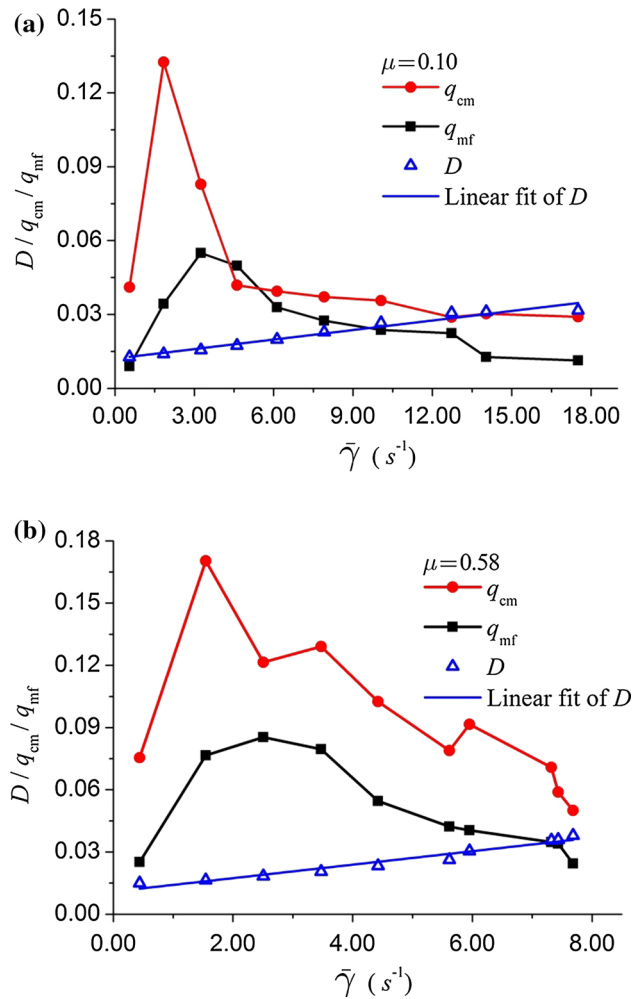


Fig. 10 Variation in $q_{v\mu}$ and D with $\bar{\gamma}$ for granular flows with different base friction coefficients: **a** base friction coefficient $\mu = 0.10$; **b** base friction coefficient $\mu = 0.58$

$\bar{\gamma}$ is defined to describe the flow regimes at different time [22]:

$$\begin{aligned} \bar{\gamma} &= \frac{\bar{U}^t}{H_{max}^t} \\ \bar{U}^t &= \langle \bar{U}(L^*, t) \rangle \\ \bar{U}(L^*, t) &= \frac{1}{H(L^*, t)} \int_0^{H(L^*, t)} U(x, z, t) dz \end{aligned} \tag{12}$$

where \bar{U}^t is the depth-averaged downstream velocity at the flowing time t ; the angle brackets denote that \bar{U}^t is computed by averaging different depth-averaged downstream velocities $\bar{U}(L^*, t)$ at different positions (different L^*) of flowing body; $H(L^*, t)$ and $U(x, z, t)$ are the thickness and downstream velocity at different positions (different L^*) of flowing body at the flowing time t , respectively; H_{max}^t is the maximum flow thickness at the flowing time t . The depth-averaged shear

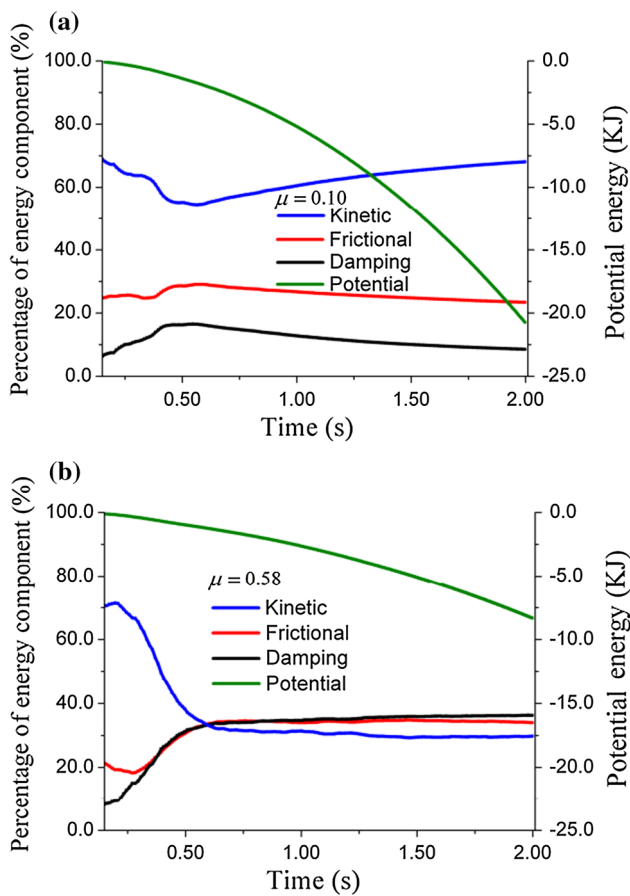


Fig. 11 Evolution of the energy components for granular flows with different base friction coefficients: **a** base friction coefficient $\mu = 0.10$; **b** base friction coefficient $\mu = 0.58$

rates are also computed every 0.20 s from the initial state to the flowing time of 2.00 s.

The thicknesses of steady uniform flows in experiments [22] and numerical simulations [25–28] are almost constant, however, the thicknesses of transient flows decrease during the flowing process. For a certain flowing time, the thicknesses at different positions of the granular bodies are also different. What is more, the velocity field in the transient flows is more complicated, the evolution of which is considered as a function of time and particle positions. Compared with the narrow change of the depth-averaged shear rate in the steady uniform flows [22], the larger increase in the particle velocity in transient flows leads to a wide range of variation in $\bar{\gamma}$ to explore the relationship between the segregation parameters and the depth-averaged shear rate.

Figure 10 shows that the segregation velocity $q_{v\mu}$ first increases to a maximum and then gradually decreases with increasing $\bar{\gamma}$. In spite of some fluctuations, this trend is consistent with the bell-shaped observations by Wiederseiner et al. [22]. Positive linear correlation exists between the diffusivity D and the depth-averaged shear rate $\bar{\gamma}$. Larger μ leads

to a faster increase in the diffusivity D with increasing $\bar{\gamma}$. This phenomenon can be explained by that the intensity of particles exchange process becomes higher. It can be concluded that both $q_{v\mu}$ and D are dependent on the depth-averaged shear rate $\bar{\gamma}$ of transient flows.

3.2.3 Energy components

Energy monitoring enhances the understanding of the particle interactions in granular materials at the microscale [42,43]. Despite an extensive number of studies in the field of dry granular flows utilizing DEM, very little work has been performed in terms of energy transformation and dissipation. This approach is extended to investigate the effect of base roughness on the behaviors of dry granular flows. The energy components considered in this paper are potential energy E_p , kinetic energy E_k , frictional energy E_f and damping energy E_d . Except for damping energy, the other different forms of energy are computed according to the reference [43]. Damping energy E_d in this paper includes the energy dissipated by particle collision E_c and the specific loss E_s :

$$E_d = E_c + E_s \tag{13}$$

The energy dissipated by particle collisions, E_c , is computed as follows [43]:

$$E_c = \sum_{t=0}^t \sum_{c=1}^{N_c} D_m du_m dt \quad (m = n, t) \tag{14}$$

where D_m is the viscous damping force, and du_m is the incremental relative displacement vector at the contact.

The local damping α operates by removing kinetic energy ΔW_t per cycle. ΔW_t is proportional to the mean kinetic W_t when the cycle is executed:

$$\frac{\Delta W_t}{W_t} = 4\alpha \quad W_t = \frac{E_{k(t)}}{N} \tag{15}$$

where $E_{k(t)}$ is the kinetic energy when the cycle is executed. The energy dissipated by the specific loss, E_s , is the total of energy loss ΔW_t [39]:

$$E_s = \sum_{t=0}^t \Delta W_t dt = \sum_{t=0}^t \frac{4\alpha E_{k(t)}}{N} dt \tag{16}$$

During the transportation process, the potential energy E_p transforms into kinetic E_k , frictional E_f , and damping energy E_d . Figure 11 illustrates the evolution of the individual percentages of the energy components accounting for the change in the potential energy of granular flows with different base friction coefficients. The change in potential energy E_p

becomes smaller when base friction is higher, which implies that the flowing distance of the particles decreases. At the beginning of transportation, the kinetic energy E_k occupies a larger amount (more than 70.0%) of the total energy conversion. The frictional energy E_f follows (approximately 25.0%) and the damping energy E_d accounts for the smallest amount (<5.0%). With the continuance of the flow of particles, the percentage of kinetic energy E_k declines significantly, whereas the two other energies (E_f and E_d) increase.

For granular flows with $\mu = 0.10$, an opposite trend for the variation of energy components appears marginally after the flowing time t (approximately 0.50 s). However, for granular flows with $\mu = 0.58$, the percentage of damping energy E_d continuously increases to transcend frictional energy E_f and kinetic energy E_k . This indicates that damping energy E_d gradually plays a significant role in the energy dissipation when base friction is greater. The decrease in the percentage of E_k also explains the decrease in the flowing distance. According to formula (16), the energy dissipated by the specific loss E_s decreases as E_k decreases. It can be considered that E_d increases mainly due to the increase in E_c (energy dissipated by particles collisions). This means that the collisions between particles increase and that contact shearing decreases relatively during the flowing process, which coincides with the change in flowing regimes.

3.2.4 Particles exchange

Particles interchange positions with their nearest neighbors during their motion, which eventually results in size segregation. Inter-particle collisions will introduce random velocities. The intensity of particles exchange process can be quantified by the random velocities. The magnitude of this “fluctuation” or “turbulence” in granular flows is defined not by the particle velocities directly, but their velocities relative to the “background velocity” [13,44,45].

In this approach, the velocity $v_i(t)$ of the selected i -th particle in the selected spherical region Ω_i can be divided into the mean velocity $\overline{v_i(t)}$ and the fluctuating part $v_i(t)'$:

$$v_i(t)' = v_i(t) - \overline{v_i(t)} \quad (17)$$

The mean velocity $\overline{v_i(t)}$ can be attained by averaging the velocities of particles surrounding the selected i -th particle in the selected spherical region Ω_i :

$$\overline{v_i(t)} = \frac{1}{n} \sum_{j=1}^n v_j(t) \quad (18)$$

$$(x_j - x_i)^2 + (y_j - y_i)^2 + (z_j - z_i)^2 \leq r^2 \quad (19)$$

where r is the radius of the selected spherical region Ω_i . In this paper, the value of 0.1 was used according to the reference [13].

With the method introduced by [19], the parameters describing granular flows along the chute are usually dimensionless. The parameter $T_i(t)$ representing the intensity of particles exchange for the selected i -th particle can be calculated from the velocity fluctuations as follows:

$$T_i(t) = (v_i(t)' / \sqrt{gr_i})^2 \quad (20)$$

where r_i is the radius of the selected i -th particle. This normalization takes into account that larger particles require a shorter path to exchange positions when the absolute displacement is the same. Dimensionless $T_i(t)$ shows how quickly this particle changes its position with respect to the surrounding particles.

By averaging $T_i(t)$ of all the particles inside the flowing body, the parameter $\overline{T(t)}$ describing the intensity of particles exchange for the entire flowing body is introduced:

$$\overline{T(t)} = \frac{1}{N} \sum_{i=1}^N T_i(t) = \frac{1}{N} \sum_{i=1}^N \frac{(v_i(t)')^2}{gr_i} \quad (21)$$

Figure 12 shows the parameter $\overline{T(t)}$ for the entire granular body with different base friction coefficients during transportation. A higher value of $\overline{T(t)}$ implies a more rapid exchange of particles and a higher rate of particle collisions. With increases in the base friction coefficient, $\overline{T(t)}$ augments significantly. For granular flows with $\mu = 0.10$ and 0.30, $\overline{T(t)}$ first increases to its maximum value and then decreases to a small value during transportation. For granular flows with $\mu = 0.50$ and 0.58, $\overline{T(t)}$ continues to increase during the flowing process. A higher base friction induces a larger $\overline{T(t)}$ inside the flowing body, namely, particles exchange their positions more frequently. This coincides with the increase in the velocity differences in Fig. 9 and larger damping energy dissipation E_d in Fig. 11.

Figure 13 shows the distribution of $T_i(t)$ inside the granular body with base friction coefficients $\mu = 0.10$ and 0.58 during transportation. The parameter $T_i(t)$ develops gradually from the particles in the front of the granular body to those in the rear. The distributions of $T_i(t)$ are significantly influenced by the base friction μ . More particles in the basal layer and front part of granular flows achieve larger $T_i(t)$, and the number of particles obtaining larger $T_i(t)$ increases obviously. It indicates that a higher base friction induces more coarse particles to exchange their positions. This explains why the centroid height of coarse particles first in the basal layer declines to a constant more quickly when base friction is higher. Considering higher rate of particle collisions and larger damping energy dissipation, it can then be postulated

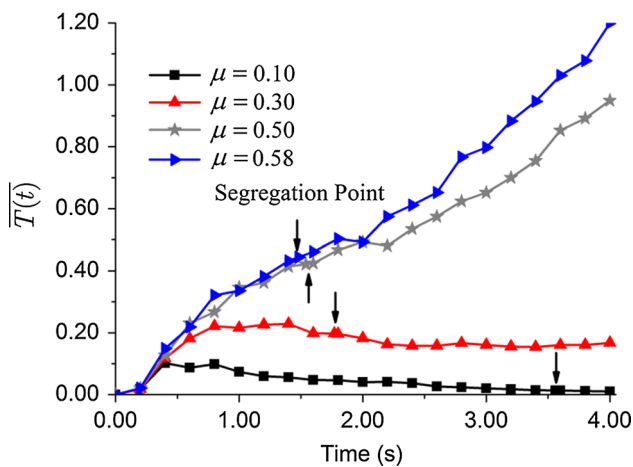


Fig. 12 Variation in the parameter $\overline{T}(t)$ describing the intensity of particles exchange for the entire granular flows with different base friction coefficients

that larger $\overline{T}(t)$ (more quick particles exchange) result from these microscopic changes with increasing base friction and then accelerate size segregation.

3.3 Mechanical effects of particle contacts

Particle segregation inside the granular body is a combination of multiple processes, such as diffusion, gravitational setting, kinetic sieving, squeeze expulsion, etc. [46]. It is necessary to analyze the effects of base roughness on particle behavior in dry granular flows from a different perspective. Savage and Lun [6] proposed the squeeze expulsion theory, that is, particles move out of their own positions into other positions above or below because force imbalances are developed inside the granular flows.

When two different sized particles are interacting, the contact force between them is the same according to the third law of Newton. However, the same contact force has different influences on the different sized particles. In consideration of this effect, a dimensionless contact force (slope-normal component) F_k^* is presented by Zhou and Ng [36] to represent the dispersive trend in the granular body:

$$F_k^* = \frac{F_{n(k)}}{F_{d(k)}} \quad (k = f, m, c) \tag{22}$$

where $F_{n(k)}$ and $F_{d(k)}$ are the slope-normal contact stress and slope-normal dispersive stress of different sized particles, respectively. $F_{n(k)}$ is defined as follows:

$$F_{n(k)} = \frac{1}{N_k} \sum_{i=1}^{N_k} \frac{F_n^i}{d_k^2} \quad (k = f, m, c) \tag{23}$$

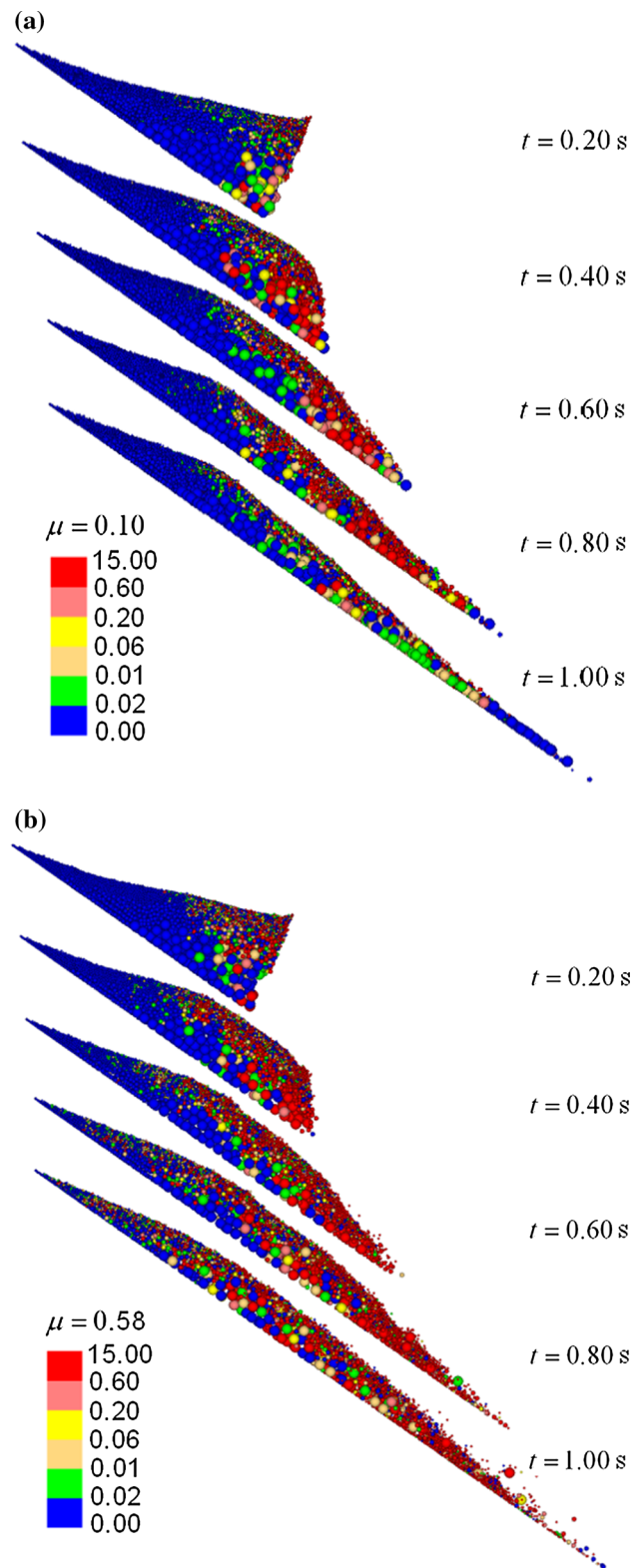


Fig. 13 The distributions of $T_i(t)$ inside the granular flows with different base friction coefficients: **a** base friction coefficient $\mu = 0.10$; **b** base friction coefficient $\mu = 0.58$

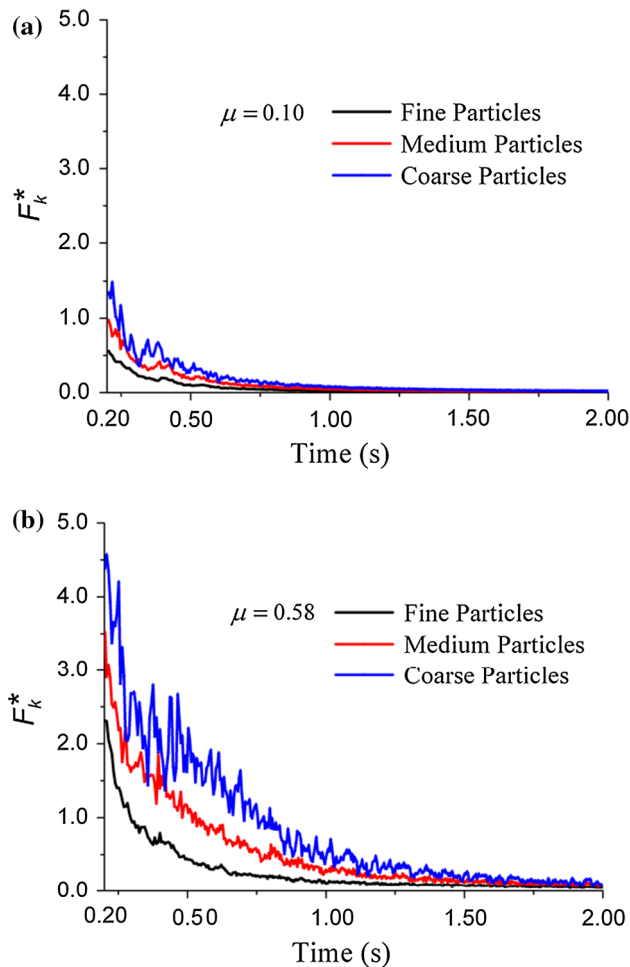


Fig. 14 Evolution of F_k^* of fine, medium and coarse particles for granular flows with different base friction coefficients: **a** base friction coefficient $\mu = 0.10$; **b** base friction coefficient $\mu = 0.58$

where F_n^i is the contact force (slope-normal component due to particle interactions) of the particle i , N_k and d_k are the number and diameter, respectively, of the fine, medium and coarse particles.

According to Bagnold's research [47], a normal dispersive stress $F_{d(k)}$ (slope-normal component) is developed inside the flowing body. Normal dispersive stress $F_{d(k)}$ results from the momentum transfer due to the exchange of particles. Similar to the gaseous molecular diffusion stress, no contacts of particles are needed to produce $F_{d(k)}$. A normal dispersive stress $F_{d(k)}$ is a repulsive stress for size segregation, which is computed as:

$$F_{d(k)} = \frac{1}{N_k} \sum_{i=1}^{N_k} F_d^i = \frac{1}{N_k} \sum_{i=1}^{N_k} \rho d_k^2 \gamma_i^2 \quad (k = f, m, c) \quad (24)$$

where F_d^i is the dispersive stress (slope-normal component due to particle interactions) of the particle i , ρ is the particle

density, d_k is the particle diameter, γ_i is the local shear rate, which is defined as v_i^n/d_k , v_i^n is the slope-normal velocity of the particle i . Therefore, Eq. (22) can be converted into another algebraic form:

$$F_k^* = \frac{F_{n(k)}}{F_{d(k)}} = \frac{\sum_{i=1}^{N_k} F_n^i}{\sum_{i=1}^{N_k} \rho d_k^2 (v_i^n)^2} \quad (k = f, m, c) \quad (25)$$

A larger value of F_k^* indicates that the contact slope-normal stress $F_{n(k)}$ has a greater contribution to dispersing the solid particles directly upward. Figure 14 shows the evolution of F_k^* of different sized particles for granular flows with different base friction coefficients. The value of F_k^* is particle-size dependent. The larger the particle size, the greater the value of F_k^* is. With base friction increasing, F_k^* decreases more slowly, and the force differences of the different sized particles become more significant. This behavior indicates that the contribution of contact normal stress $F_{n(k)}$ to dispersing different sized particles becomes notable. A higher dispersing trend is developed inside the granular bodies. From the view point of the mechanical mechanism, accelerated particle segregation can be explained by the greater contribution of $F_{n(k)}$ to dispersing particles and the more notable force differences of the different sized particles due to the higher base friction.

4 Conclusion

Based on the three-dimensional discrete element method code (Itasca PFC^{3D}), the numerical modeling of dry granular flows along a slope channel was simulated, and the effects of base roughness on size segregation and flow regimes were investigated.

The kinetic sieving and the squeeze expulsion theories were used to explain the mechanism of size segregation and how base roughness affects size segregation. The primary findings drawn from this qualitative study are as follows:

1. The size segregation and flow regimes inside the granular body are significantly influenced by base roughness. A higher base friction accelerates size segregation. However, when the base friction coefficient is higher than the ball friction coefficient, base friction has no effect on size segregation and the moving states of the granular flows. With increases in base friction, the Savage numbers are enhanced in the front part of the granular body, which indicates that the front zone of the granular body is prone to be collision dominated. The effective coordination number of granular flows becomes smaller, which means that more particles have lost contacts. More holes are developed in the granular bodies, which provide small

particles with a greater probability of percolating through the holes.

- The segregation parameters in the continuum theories [14, 18], namely the segregation velocity $q_{v\mu}$ and diffusivity D , are dependent on the depth-averaged shear rate $\bar{\gamma}$ of transient flows. Positive linear correlation exists between the diffusivity D and depth-averaged shear rate $\bar{\gamma}$, and the segregation velocity curve is bell-shaped with a maximum value.
- The kinetics of granular flows are affected by base roughness. The higher the base friction coefficient is, the larger the velocity discrepancies between different sized particles and the shorter the runout are. From the microscopic perspective, energy conversion is sensitive to base roughness. The damping energy E_d progressively plays a noticeable role in the energy dissipation due to the increasing number of particle collisions when base friction increases. The characteristics of the dissipation mechanism inside granular flows change from frictional sliding dominated to particle collision dominated.
- The parameter $\overline{T(t)}$ describing the intensity of particles exchange increases as base friction increases. This indicates that collisions between particles increase rapidly and particles interchange positions more frequently. These phenomena are the kinetic reasons why size segregation is accelerated by a higher base friction coefficient.
- From the mechanical perspective, the force acting on particle surfaces is also influenced by base roughness. The dimensionless contact force F_k^* representing the contribution of contact slope-normal stress $F_{n(k)}$ becomes larger with the growth of base friction, which reflects that a higher dispersive trend is developed inside the granular body. Force differences of different sized particles are the mechanical reasons for size segregation. Therefore, base roughness has both mechanical and kinematic effects on the particle behavior in dry granular flows.

Acknowledgments This work is supported by the National Natural Science Foundation of China (Grant Nos. 51322905, 51579193, 51509190), China Postdoctoral Science Foundation and China Scholarship Council (No. 201606270094).

Compliance with ethical standards

Conflict of interest All authors declare that they have no conflict of interest exists in the submission of this manuscript and it is compliance with ethical standards.

References

- Gray, J., Ancy, C.: Segregation, recirculation and deposition of coarse particles near two-dimensional avalanche fronts. *J. Fluid Mech.* **629**(1), 387–423 (2009)
- Gray, J., Kokelaar, B.P.: Large particle segregation, transport and accumulation in granular free-surface flows. *J. Fluid Mech.* **652**, 105–137 (2010)
- Woodhouse, M.J., Thornton, A.R., Johnson, C.G., et al.: Segregation-induced fingering instabilities in granular free-surface flows. *J. Fluid Mech.* **709**, 543–580 (2012)
- Iverson, R.M., Logan, M., LaHusen, R.G., et al.: The perfect debris flow? Aggregated results from 28 large-scale experiments. *J. Geophys. Res. Earth Surf.* **115**(F3), 1–29 (2010)
- Wang, G., Huang, R., Kamai, T., et al.: The internal structure of a rockslide dam induced by the 2008 Wenchuan (M_w 7.9) earthquake, China. *Eng. Geol.* **156**, 28–36 (2013)
- Savage, S.B., Lun, C.K.K.: Particle size segregation in inclined chute flow of dry cohesionless granular solids. *J. Fluid Mech.* **189**, 311–335 (1988)
- Tripathi, A., Khakhar, D.V.: Density difference-driven segregation in a dense granular flow. *J. Fluid Mech.* **717**, 643–669 (2013)
- Jain, N., Ottino, J.M., Lueptow, R.M.: Regimes of segregation and mixing in combined size and density granular systems: an experimental study. *Granul. Matter* **7**(2–3), 69–81 (2005)
- Pereira, G.G., Tran, N., Cleary, P.W.: Segregation of combined size and density varying binary granular mixtures in a slowly rotating tumbler. *Granul. Matter* **16**(5), 711–732 (2014)
- Tunuguntla, D.R., Bokhove, O., Thornton, A.R.: A mixture theory for size and density segregation in shallow granular free-surface flows. *J. Fluid Mech.* **749**, 99–112 (2014)
- Gray, J., Ancy, C.: Particle-size and density segregation in granular free-surface flows. *J. Fluid Mech.* **779**, 622–668 (2015)
- Brito, R., Soto, R.: Competition of Brazil nut effect, buoyancy, and inelasticity induced segregation in a granular mixture. *Eur. Phys. J. Special Top.* **179**(1), 207–219 (2010)
- Džiugys, A., Navakas, R.: The role of friction in mixing and segregation of granular material. *Granul. Matter* **11**(6), 403–416 (2009)
- Gray, J.M.N.T., Gajjar, P., Kokelaar, P.: Particle-size segregation in dense granular avalanches. *C. R. Phys.* **16**(1), 73–85 (2015)
- Gray, J., Thornton, A.R.: A theory for particle size segregation in shallow granular free-surface flows. In: *Proceedings of the Royal Society of London A: Mathematical, Physical and Engineering Sciences*, vol. 461, no. 2057, pp. 1447–1473. The Royal Society (2005)
- Gray, J., Chugunov, V.A.: Particle-size segregation and diffusive remixing in shallow granular avalanches. *J. Fluid Mech.* **569**, 365–398 (2006)
- Thornton, A.R., Gray, J., Hogg, A.J.: A three-phase mixture theory for particle size segregation in shallow granular free-surface flows. *J. Fluid Mech.* **550**, 1–26 (2006)
- Gray, J., Ancy, C.: Multi-component particle-size segregation in shallow granular avalanches. *J. Fluid Mech.* **678**, 535–588 (2011)
- Savage, S.B., Hutter, K.: The motion of a finite mass of granular material down a rough incline. *J. Fluid Mech.* **199**, 177–215 (1989)
- Greve, R., Hutter, K.: Motion of a granular avalanche in a convex and concave curved chute: experiments and theoretical predictions. *Philos. Trans. R. Soc. Lond. A Math. Phys. Eng. Sci.* **342**(1666), 573–600 (1993)
- Tai, Y.C., Noelle, S., Gray, J., et al.: Shock-capturing and front-tracking methods for granular avalanches. *J. Comput. Phys.* **175**(1), 269–301 (2002)
- Wiederseiner, S., Andreini, N., Épely-Chauvin, G., et al.: Experimental investigation into segregating granular flows down chutes. *Phys. Fluids* **23**(1), 013301 (2011)
- van der Vaart, K., Gajjar, P., Epely-Chauvin, G., et al.: Underlying asymmetry within particle size segregation. *Phys. Rev. Lett.* **114**(23), 238001 (2015)
- Marks, B., Rognon, P., Einav, I.: Grainsize dynamics of polydisperse granular segregation down inclined planes. *J. Fluid Mech.* **690**, 499–511 (2012)

25. Thornton, A., Weinhart, T., Luding, S., et al.: Modeling of particle size segregation: calibration using the discrete particle method. *Int. J. Mod. Phys. C* **23**(08), 1240014 (2012)
26. Weinhart, T., Luding, S., Thornton, A.R.: From discrete particles to continuum fields in mixtures. In: *AIP Conference Proceeding*, vol. 1542, p. 1202 (2013)
27. Staron, L., Phillips, J.C.: Segregation time-scale in bi-disperse granular flows. *Phys. Fluids* **26**(3), 033302 (2014)
28. Hill, K.M., Tan, D.S.: Segregation in dense sheared flows: gravity, temperature gradients, and stress partitioning. *J. Fluid Mech.* **756**, 54–88 (2014)
29. Maheshwari, S., Kumaran, V.: Effect of base dissipation on the granular flow down an inclined plane. *Granul. Matter* **14**(2), 209–213 (2012)
30. Kumaran, V., Bharathraj, S.: The effect of base roughness on the development of a dense granular flow down an inclined plane. *Phys. Fluids* **25**(7), 070604 (2013)
31. Shirsath, S.S., Padding, J.T., Kuipers, J.A.M., et al.: Simulation study of the effect of wall roughness on the dynamics of granular flows in rotating semicylindrical chutes. *AIChE J.* **61**(7), 2135–2177 (2015)
32. Zhao, G.F., Kazerani, T., Man, K., et al.: Numerical study of the semicircular bend dynamic fracture toughness test using discrete element models. *Sci. China Technol. Sci.* **58**(9), 1587–1595 (2015)
33. Zhang, S., Lin, P., Wang, C.L., et al.: Investigating the influence of wall frictions on hopper flows. *Granul. Matter* **16**(6), 857–866 (2014)
34. Babout, L., Grudzien, K., Maire, E., et al.: Influence of wall roughness and packing density on stagnant zone formation during funnel flow discharge from a silo: an X-ray imaging study. *Chem. Eng. Sci.* **97**, 210–224 (2013)
35. Wang, H., Tang, H.W., Yuan, S.Y., et al.: An experimental study of the incipient bed shear stress partition in mobile bed channels filled with emergent rigid vegetation. *Sci. China Technol. Sci.* **57**(6), 1165–1174 (2014)
36. Zhou, G.D., Ng, C.W.W.: Numerical investigation of reverse segregation in debris flows by DEM. *Granul. Matter* **12**(5), 507–516 (2010)
37. Zhou, G.D., Sun, Q.C.: Three-dimensional numerical study on flow regimes of dry granular flows by DEM. *Powder Technol.* **239**, 115–127 (2013)
38. Qian, J.G., Huang, M.S., Sun, H.Z.: Macro-micromechanical approaches for non-coaxiality of coarse grained soils. *Sci. China Technol. Sci.* **54**(Suppl. 1), 147–153 (2011)
39. Itasca: Particle Flow Code in 3 Dimensions. Itasca Consulting Group Inc, Minneapolis (2005)
40. Savage, S.B.: The mechanics of rapid granular flows. *Adv. Appl. Mech.* **24**, 289–366 (1984)
41. Shan, T., Zhao, J.: A coupled CFD-DEM analysis of granular flow impacting on a water reservoir. *Acta Mech.* **225**(8), 2449–2470 (2014)
42. Yang, L., Zhan, W.L.: New concept for ADS spallation target: gravity-driven dense granular flow target. *Sci. China Technol. Sci.* **58**(10), 1705–1711 (2015)
43. El Shamy, U., Denissen, C.: Microscale characterization of energy dissipation mechanisms in liquefiable granular soils. *Comput. Geotech.* **37**(7), 846–857 (2010)
44. Campbell, C.S.: Granular material flows—an overview. *Powder Technol.* **162**(3), 208–229 (2006)
45. Kuhn, M.R.: Structured deformation in granular materials. *Mech. Mater.* **31**(6), 407–429 (1999)
46. Zhou, G.D., Law, R.P.H., Ng, C.W.W.: The mechanisms of debris flow: a preliminary study. In: Hamza, M., Shahien, M., El-Mossallamy, Y. (eds.) *The Proceedings of the 17th International Conference on Soil Mechanics and Geotechnical Engineering: The Academia and Practice of Geotechnical Engineering*, vol. 2, pp. 1570–1573 (2009)
47. Bagnold, R.A.: Experiments on a gravity-free dispersion of large solid spheres in a Newtonian fluid under shear. *Proc. R. Soc. Lond. Ser. A* **225**(1160), 49–63 (1954)